PHYSICAL REVIEW D **85,** 083522 (2012)

Sterile neutrino models and nonminimal cosmologies

Elena Giusarma,[1] Maria Archidiacono,[2] Roland de Putter,[1,3] Alessandro Melchiorri,[2] and Olga Mena[1]
[1]*IFIC, Universidad de Valencia-CSIC, 46071, Valencia, Spain*
[2]*Physics Department and INFN, Universita' di Roma "La Sapienza", Ple. Aldo Moro 2, 00185, Rome, Italy*
[3]*ICC, University of Barcelona (IEEC-UB), Marti i Franques 1, Barcelona 08028, Spain*
(Received 28 December 2011; published 23 April 2012)

Cosmological measurements are affected by the energy density of massive neutrinos. We extend here a recent analysis of current cosmological data to nonminimal cosmologies. Several possible scenarios are examined: a constant $w \neq -1$ dark energy equation of state, a nonflat universe, a time-varying dark energy component and coupled dark matter-dark energy universes or modified gravity scenarios. When considering cosmological data only, (3 + 2) massive neutrino models with ~0.5 eV sterile species are allowed at 95% confidence level. This scenario has been shown to reconcile reactor, LSND and MiniBooNE positive signals with null results from other searches. Big bang nucleosynthesis bounds could compromise the viability of (3 + 2) models if the two sterile species are fully thermalized states at decoupling.

DOI: 10.1103/PhysRevD.85.083522 PACS numbers: 98.80.−k, 95.85.Sz, 98.70.Vc, 98.80.Cq

I. INTRODUCTION

Solar, atmospheric, reactor, and accelerator neutrinos have provided compelling evidence for the existence of neutrino oscillations, implying nonzero neutrino masses (see Ref. [1] and references therein). The present data require the number of massive neutrinos to be equal or larger than two, since there are at least two mass squared differences ($\Delta m^2_{\rm atmos}$ and $\Delta m^2_{\rm solar}$) driving the atmospheric and solar neutrino oscillations, respectively. Unfortunately, oscillation experiments only provide bounds on the neutrino mass squared differences, i.e., they are not sensitive to the overall neutrino mass scale.

Cosmology provides one of the means to tackle the absolute scale of neutrino masses. Neutrinos can leave key signatures in several cosmological data sets. The amount of primordial relativistic neutrinos changes the epoch of the matter-radiation equality, leaving an imprint on both cosmic microwave background (CMB) anisotropies (through the so-called integrated Sachs-Wolfe effect) and on structure formation, while nonrelativistic neutrinos in the recent Universe suppress the growth of matter density fluctuations and galaxy clustering, see Ref. [2]. Cosmology can therefore weigh neutrinos, providing an upper bound on the sum of the three active neutrino masses, $\sum m_\nu \sim 0.58$ eV at 95% CL [3]. The former bound is found when CMB measurements from the Wilkinson Microwave Anisotropy Probe (WMAP) are combined with measurements of the distribution of galaxies (SDSS-II-BAO) and of the Hubble constant H_0 (HST)[1] in the assumption of a flat universe with a cosmological constant, i.e., a ΛCDM cosmology.

There is no fundamental symmetry in nature forcing a definite number of right-handed (sterile) neutrino species, as those are allowed in the standard model fermion content. Indeed, cosmological probes have been extensively used to set bounds on the relativistic energy density of the universe in terms of the effective number of neutrinos $N_\nu^{\rm eff}$ (see, for instance, Refs. [3–9]. If the effective number of neutrinos $N_\nu^{\rm eff}$ is larger than the standard model prediction of $N_\nu^{\rm eff} = 3.046$ at the big bang nucleosynthesis (BBN) era, the relativistic degrees of freedom, and, consequently, the Hubble expansion rate will also be larger causing weak interactions to become uneffective earlier. This will lead to a larger neutron-to-proton ratio and will change the standard BBN predictions for light element abundances. Combining Deuterium and H^4e data, the authors of Ref. [6] found $N_\nu^{\rm eff} = 3.1^{+1.4}_{-1.2}$ at 95% confidence level (CL).

Models with one additional ~1 eV massive sterile neutrino, i.e., the so-called (3 + 1) models, were introduced to explain LSND short baseline antineutrino data [10] by means of neutrino oscillations. A much better fit to short baseline appearance data and, to a lesser extent, to disappearance data, is provided by models with two sterile neutrinos (3 + 2) [11,12] which can also explain both the MiniBooNE neutrino [13] and antineutrino data [14] if *CP* violation is allowed [15]. More recently, a combined analysis including the new reactor antineutrino fluxes [16,17] has shown that (3 + 2) models provide a very good fit to short baseline data [18]. While these models with extra sterile species show some tension with BBN bounds on $N_\nu^{\rm eff}$, the extra sterile neutrinos do not necessarily have to feature thermal abundances at decoupling, see Refs. [19,20], where the usual full thermalization scenario for the sterile neutrino species was not assumed. Up-to-date cosmological constraints on massive sterile and active neutrino species have been presented in Refs. [21,22] in the context of a ΛCDM universe. It is well-known that bounds on active neutrino species are relaxed if the dark energy equation of state is different

[1]For other recent analyses, see also Refs. [4,5].

from -1 [23–25] and/or interactions between the dark matter and dark energy sectors are switched on [26,27]. In the same line, the authors of Ref. [28] have found that in models with nonzero curvature and two extra sterile neutrinos the cosmological constant scenario is ruled out at 95% CL.

Here we extend the minimal cosmological scenario considered in our previous study [22] and compute the bounds on the masses of the active and the sterile neutrino states as well as on the number of sterile states in the presence of a constant equation of state $w \neq 1$, a time-varying dark energy fluid, a nonvanishing curvature component and interactions among the dark sectors. The paper is organized as follows. Section II describes the details of the analysis carried out here, including the cosmological parameters and datasets. The four different cosmological scenarios explored here are analyzed and the most important degeneracies among the neutrino parameters are carefully explored. Section III summarizes our main results and conclusions.

II. COSMOLOGICAL CONSTRAINTS

Here we present the constraints from current data on the active neutrino masses and on the sterile neutrino thermal abundance and masses in different cosmological scenarios. Cosmological data is only sensitive the effective number of neutrino species, that is, three active neutrinos plus N_{ν_s} sterile ones ($N_\nu^{\rm eff} = 3 + N_{\nu_s}$) and to the total amount of dark matter in the form of massive neutrinos

$$\Omega_\nu^{\rm eff} h^2 = \Omega_{\nu_s} h^2 + \Omega_\nu h^2, \tag{1}$$

$$\frac{N_\nu^{\rm eff} m_\nu^{\rm eff}}{94\ {\rm eV}} = \frac{(3 m_\nu + N_{\nu_s} m_{\nu_s})}{94\ {\rm eV}}, \tag{2}$$

that is, to the active plus sterile neutrino mass-energy densities. However, the only motivation for the existence of additional, sterile massive neutrinos comes from neutrino oscillation experiments, which are sensitive to the number of sterile species and to the mass squared differences among the neutrino mass eigenstates. Therefore, in order to test the so-called (3 + 2) sterile neutrino models suggested by neutrino oscillation data, we choose a parameter space which considers three active neutrino masses and N_{ν_s} sterile neutrino species with masses m_{ν_s} separately, accordingly to what has been done previously in the literature [19,22]. We believe this approach is correct because it directly tests the models suggested by neutrino oscillation data: cosmological constraints become meaningful for neutrino model building.

We have modified the Boltzmann CAMB code [29] incorporating the extra massive sterile neutrino parameters and extracted cosmological parameters from current data using a Monte Carlo Markov Chain (MCMC) analysis based on the publicly available MCMC package COSMOMC [30]. We consider here four possible scenarios: the wCDM model in which we include the possibility of a dark energy equation of state parameter w different from -1, the $w(a)$CDM model in which we assume an equation of state evolving with redshift, the Ω_kCDM model where we allow the spatial curvature of the universe to vary, and the model in which an interaction among the dark matter and dark energy sectors is switched on, the ξCDM model. These scenarios are an extension of the minimal cosmological model plus three (N_{ν_s}) active (sterile) massive neutrino species. We consider subsets of the following parameters:

$$\{\omega_b, \omega_c, \Theta_s, \tau, n_s, \log[10^{10} A_s], m_\nu, m_{\nu_s}, N_{\nu_s}, w(w_0), w_a, \Omega_k, \xi\},$$

where $\omega_b \equiv \Omega_b h^2$ and $\omega_c \equiv \Omega_c h^2$ are the physical baryon and cold dark matter densities, Θ_s is the ratio between the sound horizon and the angular diameter distance at decoupling, τ is the optical depth, n_s is the scalar spectral index, A_s is the amplitude of the primordial spectrum, m_ν is the active neutrino mass, m_{ν_s} is the sterile neutrino mass and N_{ν_s} is the number of thermalized sterile neutrino species,[2] w is the dark energy equation of the state parameter, Ω_k is the curvature parameter, ξ is the dimensionless parameter which encodes the dark matter-dark energy interaction, and w_0, w_a are parameters related to the dark energy equation of state. Table I specifies the priors considered on the different cosmological parameters. In all cases in which $w \neq -1$ we have considered the effect of dark energy perturbations, fixing the dark energy speed of sound $c_s^2 = 1$.

TABLE I. Flat priors for the cosmological parameters considered here.

Parameter	Prior
$\Omega_b h^2$	$0.005 \rightarrow 0.1$
$\Omega_c h^2$	$0.01 \rightarrow 0.99$
Θ_s	$0.5 \rightarrow 10$
τ	$0.01 \rightarrow 0.8$
n_s	$0.5 \rightarrow 1.5$
$\ln(10^{10} A_s)$	$2.7 \rightarrow 4$
m_{ν_s} [eV]	$0 \rightarrow 3$
m_ν [eV]	$0 \rightarrow 3$
N_{ν_s}	$0 \rightarrow 6$
$w(w_0)$	$-2 \rightarrow 0$
w_a	$-1 \rightarrow 1$
Ω_k	$-0.02 \rightarrow 0.03$
ξ	$-2 \rightarrow 0.$

Our basic data set is the seven—year WMAP data [3,31] (temperature and polarization) with the routine for computing the likelihood supplied by the WMAP team. We consider two cases: we first analyze the WMAP data together with the luminous red galaxy clustering results from SDSS-II (Sloan Digital Sky Survey) [32] and with a

[2]We assume that both active and sterile neutrinos have a degenerate mass spectra.

prior on the Hubble constant from HST (Hubble Space Telescope) [33], referring to it as the "run1" case. We then include with these data sets Supernova Ia Union Compilation 2 data [34], and we will refer to this case as "run2." In addition, we also add to the previous data sets the BBN measurements of the H^4e abundance, considering separately helium fractions of $Y_p^1 = 0.2561 \pm 0.0108$ (see Ref. [35]) and of $Y_p^2 = 0.2565 \pm 0.0010(\text{stat}) \pm 0.0050(\text{syst})$ from Ref. [36]. Finally, we also consider the Deuterium abundance measurements $\log(D/H) = -4.56 \pm 0.04$ from Ref. [37].

Since the CMB data we are considering are not significantly constraining the amount of primordial Helium abundance, we fix it to the value $Y_p = 0.24$, consistent with current observations. Then we use the MCMC chains from each different run and perform importance sampling obtaining the predicted values for Y_p and $\log(D/H)$ with an interpolation routine using a grid of the public available PARTHENOPE BBN code (see [38]) for each point (ω_b, $N_\nu^{\rm eff} = 3 + N_{\nu_s}$) of a given cosmological model, as in [39].

In the following, we will present the cosmological constraints on the masses of the active and the sterile neutrino states as well as on the number of sterile states for different cosmological scenarios, namely, a universe with a constant equation of state $w \neq -1$, a universe with a time-varying dark energy fluid, a universe with a nonvanishing curvature component and a universe with interacting dark matter-dark energy sectors.

A. wCDM cosmology

We first consider a cosmological model including standard cold dark matter and a dark energy fluid characterized by a constant equation of state w. We consider the following set of parameters:

$$\{\omega_b, \omega_c, \Theta_s, \tau, n_s, \log[10^{10}A_s], m_\nu, m_{\nu_s}, N_{\nu_s}, w\}. \quad (3)$$

Table II shows the one-dimensional (1D) marginalized 95% CL bounds on N_{ν_s}, m_{ν_s}, m_ν and the active plus sterile neutrino mass-energy densities $\Omega_\nu^{\rm eff}h^2$ using the two combinations of data sets described above. Note that the addition of SNIa data affects only the number of massive sterile neutrino species, and not their masses. The bounds obtained in a ΛCDM scenario, see Table VI in Appendix A [22] are slightly relaxed when the dark energy equation of state is allowed to vary. There is a strong and very well-known degeneracy in the $m_\nu - w$ plane (and therefore also in the $m_{\nu_s} - w$ plane) as first noticed in Ref. [23]. Cosmological neutrino mass bounds become weaker if the dark energy equation of state is taken as a free parameter. If w is allowed to vary, the cold dark matter mass-energy density Ω_c can take very high values, as required when the neutrino mass is increased, in order to have the same matter power spectrum. We can observe this degeneracy in the upper panel of Fig. 1. Notice that a similar degeneracy will appear in the $m_{\nu_s} - w$ plane, since we are splitting here the total amount of hot dark matter into three active plus N_{ν_s} sterile species. There exists also a degeneracy between the number of sterile neutrino species and the dark energy equation of state, see Fig. 1 (lower panel). Sub-eV massive sterile neutrino species may be quasirelativistic states at decoupling. One of the main effects of N_{ν_s} comes from the change of the epoch of the radiation matter equality, and consequently, from the shift of the CMB acoustic peaks, see Ref. [40] for a detailed study. The position of acoustic peaks is given by the so-called acoustic scale θ_A, which reads

$$\theta_A = \frac{r_s(z_{\rm rec})}{r_\theta(z_{\rm rec})}, \quad (4)$$

where $r_\theta(z_{\rm rec})$ and $r_s(z_{\rm rec})$ are the comoving angular diameter distance to the last scattering surface and the sound horizon at the recombination epoch $z_{\rm rec}$, respectively. Although $r_\theta(z_{\rm rec})$ almost remains the same for different values of N_{ν_s}, $r_s(z_{\rm rec})$ becomes smaller when N_{ν_s} is increased. Thus the positions of acoustic peaks are shifted to higher multipoles (smaller angular scales) by increasing the value of N_{ν_s} [41]. A dark energy component with $w > -1$ will decrease the comoving angular diameter distance to the last scattering surface $r_\theta(z_{\rm rec})$, shifting the positions of the CMB acoustic peaks to larger angular scales, i.e., to lower multipoles ℓ, compensating, therefore, the effect induced by an increase of N_{ν_s}. Notice as well that the degeneracy in the $N_{\nu_s} - w$ plane can be predictable from that existing in the $m_{\nu_s} - w$ plane, since cosmological data is sensitive to the total amount of hot dark matter $(3m_\nu + N_{\nu_s}m_{\nu_s})$ and if the equation of state and m_{ν_s} are positively correlated the number of sterile neutrinos N_{ν_s} and the equation of state must be negatively correlated.

TABLE II. 1D marginalized 95% CL bounds on N_{ν_s}, m_{ν_s}, m_ν and the active plus sterile neutrino mass-energy densities $\Omega_\nu^{\rm eff}h^2$ using the two combinations of data sets described in the text (r1 refers to "run1" and r2 refers to "run2") for the wCDM cosmology. We also show the constraints after combining the results of run2 with those coming from different measurements of BBN light element abundances.

Parameter	95% CL (r1)	95% CL (r2)	Y_p^1	Y_p^2	$Y_p^1 + D$	$Y_p^2 + D$
N_{ν_s}	<4.4	<3.9	<2.3	<1.6	<1.6	<1.3
m_ν [eV]	<0.34	<0.31	<0.25	<0.23	<0.23	<0.23
m_{ν_s} [eV]	<0.51	<0.57	<0.68	<0.71	<0.75	<0.75
$\Omega_\nu^{\rm eff}h^2$	<0.035	<0.034	<0.025	<0.019	<0.020	<0.018

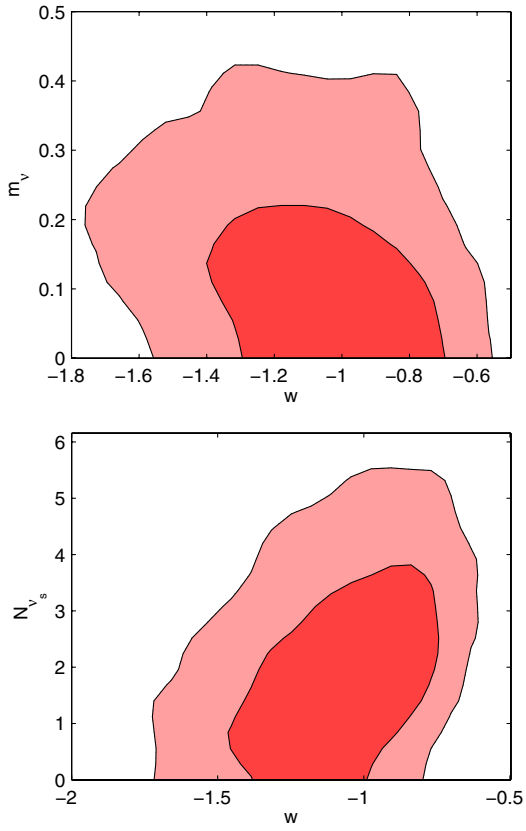

FIG. 1 (color online). The upper panel shows the 68% and 95% CL bounds from run1 in the plane $w - m_\nu$. The mass of the active neutrinos is in eV. The lower panel depicts the 68% and 95% CL contours in the plane $w - N_{\nu_s}$ for a constant dark energy equation of state.

We have also computed the constraints after combining the results of run2 with those coming from different measurements of BBN light element abundances, see Table II. The bounds on N_{ν_s} obtained in a wCDM cosmology when adding BBN constraints are very similar to those obtained in a ΛCDM scenario [22]. The limits on the active and neutrino masses are mildly relaxed.

B. $w(a)$CDM cosmologies

We also consider a time-varying equation of state with a parameterization that has been extensively explored in the literature [42–45]

$$w(a) = w_0 + w_a(1 - a). \tag{5}$$

We consider the following set of parameters:

$$\{\omega_b, \omega_c, \Theta_s, \tau, n_s, \log[10^{10}A_s], m_\nu, m_{\nu_s}, N_{\nu_s}, w_0, w_a\}. \tag{6}$$

Table III shows the 1D marginalized 95% CL bounds on N_{ν_s}, m_{ν_s}, m_ν and the active plus sterile neutrino mass-energy densities $\Omega_\nu^{\rm eff}h^2$ using the two combinations of data sets used along this manuscript. The addition of SNIa data does not improve at all the constraints from run1. There exist large degeneracies in the $m_\nu - w_0$ plane (and consequently, in the $m_{\nu_s} - w_0$ and $N_{\nu_s} - w_0$ planes). These degeneracies are identical to the wCDM cosmology ones, and therefore we will not illustrate them here to avoid redundancy. We show instead the mild degeneracy in the $N_{\nu_s} - w_a$ plane, see Fig. 2. In this case, an increase of N_{ν_s} will be compensated by a decrease of w_a. The BBN bounds combined with the run2 constraints on the neutrino parameters are also depicted in Table III.

C. Nonflat Ω_kCDM cosmologies

We also explore here the constraints in nonflat cosmologies. We consider the following set of parameters:

$$\{\omega_b, \omega_c, \Theta_s, \tau, n_s, \log[10^{10}A_s], m_\nu, m_{\nu_s}, N_{\nu_s}, \Omega_k\}. \tag{7}$$

Current CMB measurements combined with SNIa and BAO data, give the constraint $\Omega_k = -0.0057^{+0.0067}_{-0.0068}$ [3]. Table IV shows the 1D marginalized 95% CL bounds on N_{ν_s}, m_{ν_s}, m_ν and the active plus sterile neutrino mass-energy densities using the two combinations of data sets considered here. The bounds are very similar to those obtained in the other two cosmological models explored above.

Figure 3 shows the existing degeneracies between the curvature energy density and the number of massive sterile neutrino species N_{ν_s} and between the curvature and the mass of the active neutrino species (identical to the existing one with the mass of the sterile neutrino species). In an open universe with $\Omega_k > 0$ the comoving angular diameter distance to the last scattering surface $r_\theta(z_{\rm rec})$ will be higher, shifting the positions of the CMB acoustic peaks to smaller angular scales, i.e., to larger multipoles ℓ, which can be compensated with a larger dark matter energy density which will allow for higher neutrino masses. At the same time a higher dark matter energy density will decrease the height of the acoustic peaks, features which can be compensated by a larger number of sterile neutrino species.

TABLE III. As Table II, but for the $w(a)$CDM cosmology.

Parameter	95% CL(r1)	95% CL(r2)	Y_p^1	Y_p^2	$Y_p^1 + D$	$Y_p^2 + D$
N_{ν_s}	<4.5	<4.4	<2.6	<1.7	<1.7	<1.4
m_ν [eV]	<0.33	<0.31	<0.26	<0.23	<0.22	<0.22
m_{ν_s} [eV]	<0.49	<0.48	<0.58	<0.66	<0.73	<0.72
$\Omega_\nu^{\rm eff}h^2$	<0.033	<0.032	<0.025	<0.019	<0.020	<0.018

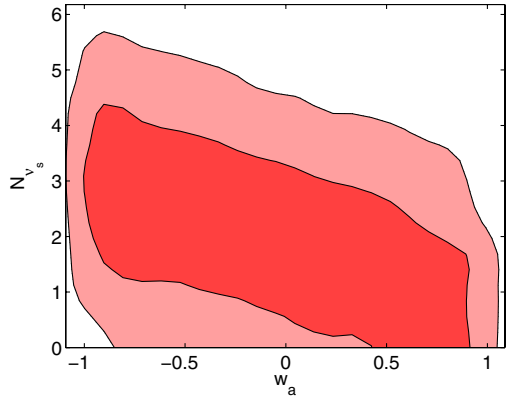

FIG. 2 (color online). 68% and 95% CL contours arising from run1 in the plane $w - N_{\nu_s}$ for the $w(a)$CDM cosmology.

Table IV also shows the constraints arising from BBN measurements combined with run2 bounds.

D. Coupled ξCDM cosmologies and modified gravity scenarios

Interactions within the dark sectors, i.e., between cold dark matter and dark energy, are still allowed by observations (see Ref. [46] and references therein). We parametrize the dark matter-dark energy interactions at the level of the stress-energy tensor conservation equations, introducing an energy momentum exchange of the following form [47]:

$$\nabla_\mu T^\mu_{(c)\nu} = Q_\nu; \qquad \nabla_\mu T^\mu_{(de)\nu} = -Q_\nu, \tag{8}$$

with

$$Q_\nu = \xi \mathcal{H} \rho_{de} u^c_\nu / a \qquad \text{or} \qquad Q_\nu = \xi \mathcal{H} \rho_{de} u^{de}_\nu / a, \tag{9}$$

where $u^{c(de)}_\nu$ is the cold dark matter (dark energy) four velocity and ξ is a dimensionless coupling, considered negative in order to avoid early time nonadiabatic instabilities [27]. In general, coupled models with Q_ν proportional to u^{de}_ν are effectively modified gravity models. We consider the following set of parameters:

$$\{\omega_b, \omega_c, \Theta_s, \tau, n_s, \log[10^{10} A_s], m_\nu, m_{\nu_s}, N_{\nu_s}, w, \xi\}. \tag{10}$$

Interactions between the dark matter and dark energy sectors can relax the bounds on the active neutrino masses [26,27] since, for negative couplings, the power spectrum increases due the higher matter-energy density when

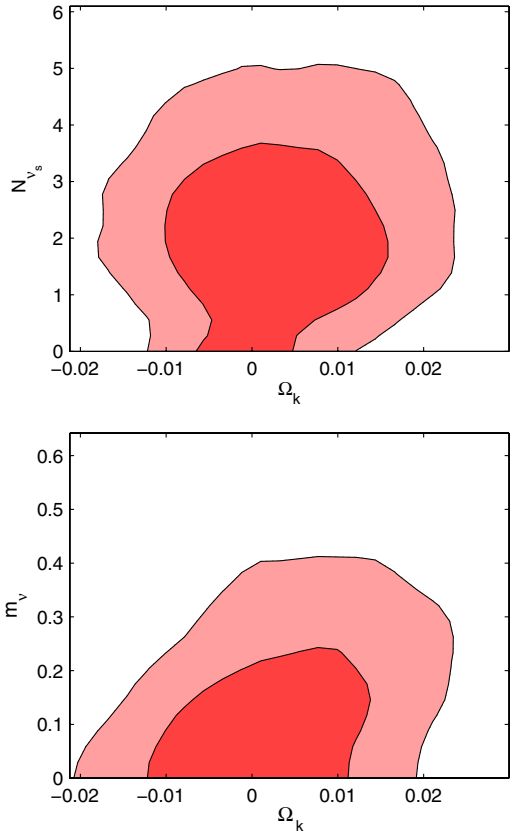

FIG. 3 (color online). The upper panel shows the 68% and 95% CL bounds from run1 in the $\Omega_k - N_{\nu_s}$ plane. The lower plane shows the analogous in the $\Omega_k - m_\nu$ plane. The masses of the active neutrinos are in eV.

$\xi < 0$. Such a power enhancement effect (induced by the presence of a coupling) can be compensated by adding massive neutrinos in the game, which will suppress the matter power spectrum. Therefore, there exists a well-known $m_\nu - \xi$ degeneracy. Here we illustrate an additional degeneracy, which is closely related to the previous one: the one existing in the $N_{\nu_s} - \xi$ plane. Figure 4 shows the existing degeneracy among the coupling ξ and the number of sterile massive neutrino species for a coupling term proportional to u^c_ν (identical results are obtained for the case proportional to u^{de}_ν). As first noticed in Ref. [27] a huge degeneracy is present between the coupling ξ and the mass-energy density of cold dark matter ω_c, with the former two quantities having positive correlations. In a universe with a negative dark coupling ξ, the matter content in the

TABLE IV. As Table II, but for the Ω_kCDM cosmology.

Parameter	95% CL(r1)	95% CL(r2)	Y^1_p	Y^2_p	$Y^1_p + D$	$Y^2_p + D$
N_{ν_s}	<4.3	<3.8	<2.4	<1.7	<1.7	<1.4
m_ν [eV]	<0.34	<0.31	<0.24	<0.22	<0.22	<0.21
m_{ν_s} [eV]	<0.45	<0.52	<0.70	<0.72	<0.77	<0.75
$\Omega^{\rm eff}_\nu h^2$	<0.032	<0.031	<0.026	<0.020	<0.021	<0.018

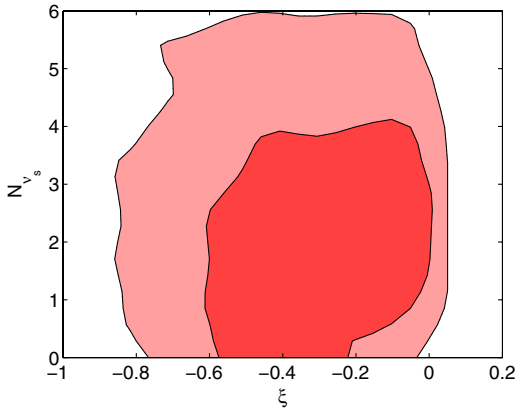

FIG. 4 (color online). 68% and 95% CL bounds arising from the run1 analysis in the plane $\xi - N_{\nu_s}$ for a universe with an interacting dark matter-dark energy fluid.

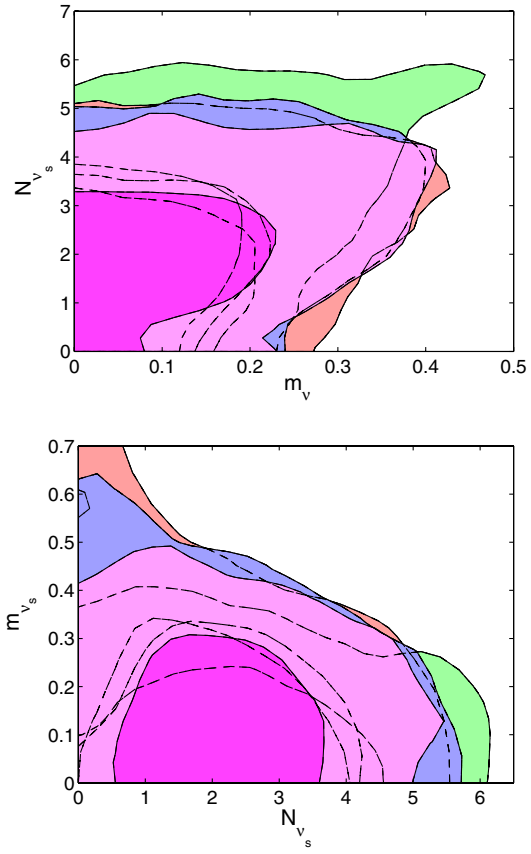

FIG. 5 (color online). The upper panel shows the 68% and 95% CL bounds from run1 in the $m_\nu - N_{\nu_s}$ plane. The lower plane shows the analogous in the $N_{\nu_s} - m_{\nu_s}$ plane. The masses of the sterile and active neutrinos are both in eV. Red, blue, magenta and green contours denote wCDM, $w(a)$CDM, Ω_kCDM and ξCDM cosmologies, respectively.

past is higher than in a standard ΛCDM scenario, since the cold dark matter and dark energy densities read

$$\Omega_c = \Omega_c^0 a^{-3} + \Omega_{de}^0 \frac{\xi}{(w + \frac{\xi}{3})}(1 - a^{-3(w+\xi/3)})a^{-3}; \quad (11)$$

$$\Omega_{de} = \Omega_{de}^0 a^{-3(1+w+\xi/3)}, \quad (12)$$

with $\Omega_{c,de}^0$ the current cold dark matter (dark energy) mass-energy densities. Therefore, the amount of intrinsic dark matter needed—that is, not including the contribution of dark energy through the coupling term—should decrease as the dark coupling becomes more and more negative. Therefore, the number of effective neutrino species should also decrease as the coupling gets more negative to leave unchanged both the matter-radiation equality epoch and the first CMB peak heigh. Table V shows the analogous to previous sections but for the coupled case. Notice that the bounds on the number of massive sterile neutrinos arising from run1 and run2 analyses are milder than those obtained in the previous cosmologies, due to the degeneracy between the coupling ξ and N_{ν_s}.

III. DISCUSSION AND CONCLUSIONS

Neutrino oscillation experiments indicate that neutrinos have nonzero masses and open the possibility for a number of extra sterile neutrino species. LSND and MiniBooNE antineutrino data require these extra sterile species to be massive. Much effort has been devoted in the literature to constrain the so-called (3 + 1) (three active plus one sterile) and (3 + 2) (three active plus two sterile). Recently, global fit analyses incorporating new reactor antineutrino fluxes have shown that (3 + 2) models with $0.5 - 1$ eV sterile species provide a very good fit to short baseline data. Cosmology can set bounds on both the total number of neutrinos and the amount of mass-energy density in the form of neutrinos. In order to be able to make direct comparisons to the results reported by neutrino oscillation experiments, we parametrize the total amount of hot dark matter as three active degenerate neutrinos with mass m_ν and N_{ν_s} sterile neutrino species with degenerate masses m_{ν_s}. This approach is the one considered previously in the literature and is extremely useful for

TABLE V. As Table II, but for the ξCDM cosmology.

Parameter	95% CL(r1)	95% CL(r2)	Y_p^1	Y_p^2	$Y_p^1 + D$	$Y_p^2 + D$
N_{ν_s}	<5.2	<4.7	<2.4	<1.7	<1.8	<1.4
m_ν [eV]	<0.34	<0.33	<0.21	<0.21	<0.20	<0.20
m_{ν_s} [eV]	<0.35	<0.38	<0.47	<0.51	<0.49	<0.49
$\Omega_\nu^{\rm eff} h^2$	<0.030	<0.026	<0.019	<0.016	<0.016	<0.014

TABLE VI. 1D marginalized 95% CL bounds on N_{ν_s}, m_{ν_s}, m_ν and the active plus sterile neutrino mass-energy densities $\Omega_\nu^{\rm eff}h^2$ using the two combinations of data sets described in the text (r1 refers to run1 and r2 refers to run2) for a ΛCDM cosmology, see Ref. [22]. We also show the constraints after combining the results of run2 with those coming from different measurements of BBN light element abundances.

Parameter	95% CL(r1)	95% CL(r2)	Y_p^1	Y_p^2	$Y_p^1 + D$	$Y_p^2 + D$
N_{ν_s}	<4.1	<3.2	<2.3	<1.7	<1.7	<1.4
m_ν [eV]	<0.30	<0.20	<0.17	<0.15	<0.15	<0.15
m_{ν_s} [eV]	<0.46	<0.50	<0.62	<0.67	<0.69	<0.68
$\Omega_\nu^{\rm eff}h^2$	<0.030	<0.023	<0.021	<0.017	<0.017	<0.015

combinations of short baseline and cosmological data sets. The relation between the parameters of interest, and the parameter combinations mainly constrained by cosmology (namely, the total number of neutrino species, and the average mass) can be used to better understand the degeneracies we find. We discuss this in detail in Appendix B.

We have explored here the current constraints on these parameters in natural extensions of the minimal ΛCDM cosmology. Namely, we have explored the neutrino constraints in scenarios without a cosmological constant as the dark energy fluid, with a nonvanishing curvature, or with coupled dark matter-dark energy fluids. Figure 5 summarizes our results in the $m_\nu - N_{\nu_s}$ and $N_{\nu_s} - m_{\nu_s}$ planes. Notice that models with two massive $0.5 - 1$ eV sterile neutrinos plus three sub-eV active states are perfectly allowed at 95% CL by current cosmic microwave background, galaxy clustering and Supernovae Ia data. Interestingly, these models are precisely the ones which, with the new reactor fluxes prediction, improve considerably the global fit to short baseline data. While we have not checked directly the results of Ref. [28] in which models with nonzero curvature and two extra sterile neutrinos seem to exclude $w = -1$ at 95% CL, it seems plausible that nonstandard ΛCDM cosmologies with sterile neutrino species provide also a very good fit to cosmological data. Big bang nucleosynthesis constraints could compromise the viability of these models if the two sterile neutrino states are fully thermal. If the BBN constraints are obtained using the helium fraction measurements Y_p from [35] exclusively, two extra sterile neutrino states are perfectly allowed ($N_{\nu_s} < 2.3$ at 95% CL). Even after combining these data with Deuterium measurements, two massive neutrino states are only marginally excluded ($N_{\nu_s} < 1.7$ at 95% CL). The tightest bound on the number of sterile neutrino species arises when helium measurements from Ref. [36] are combined with Deuterium data. Further developments in BBN determinations of light element abundances may have a large impact in further constraining the number of sterile neutrino species N_{ν_s}.

ACKNOWLEDGMENTS

R. d. P. is supported by FP7-IDEAS-Phys.LSS 240117. O. M. is supported by AYA2008-03531 and the Consolider Ingenio project CSD2007-00060. We acknowledge support from the MICINN-INFN agreements ACI2009-1049, ACI-D-2011-0783 and INFN2008-016.

APPENDIX A: ΛCDM RESULTS

Table VI summarizes the main results obtained in [22] for a standard ΛCDM cosmology, for the sake of comparison with the results obtained within the other cosmological scenarios explored here. Despite the fact that the constraints on N_{ν_s}, m_{ν_s} and m_ν for the other scenarios are always similar to the ones obtained within a ΛCDM model, adding extra parameters relaxes the constraints: notice that the bounds on the active plus sterile neutrino mass-energy densities $\Omega_\nu^{\rm eff}$, that is the quantity to which cosmological data is sensitive to, are always weaker when enlarged versions of the minimal ΛCDM are considered.

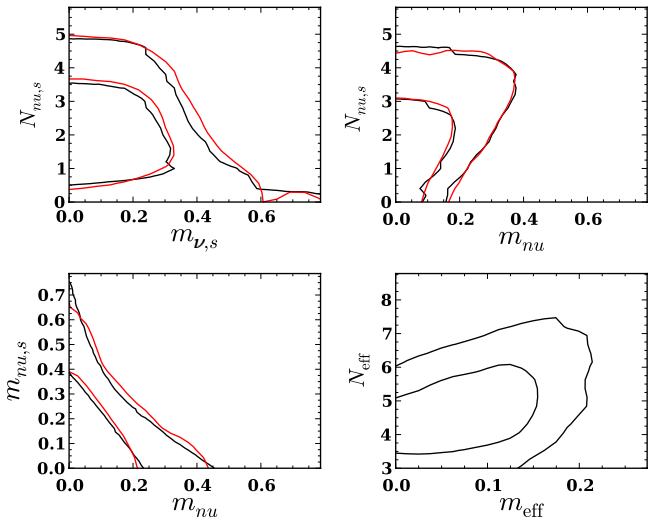

FIG. 6 (color online). *Bottom Right:* Likelihood contours (68% and 95% CL) for the effective, total number of neutrino species $N_{\rm eff}$ and the average, or effective, neutrino mass $m_{\rm eff}$. The run1 combination of data sets is used. *Other Panels:* Using the fact that current cosmological data are only sensitive to $N_{\rm eff}$ and $m_{\rm eff}$, constraints on m_ν, m_{ν_s} and N_{ν_s} are derived (black). The red contours show the contours (from [22]) obtained from a MCMC analysis of the full neutrino parameter space, which agree very well. ΛCDM parameters are marginalized over in all cases.

APPENDIX B: UNDERSTANDING PARAMETER DEGENERACIES

In this article, we study cosmological constraints on m_ν, m_{ν_s} and N_{ν_s} because these are the physically interesting parameters and are closely related to particle physics experiment. However, it is well-known that (current) cosmological data only have the capacity to constrain two independent combinations of neutrino parameters, which can be taken to be the total number of species

$$N_{\rm eff} = 3 + N_{\nu_s} \tag{B1}$$

and the average, or effective, neutrino mass

$$m_{\rm eff} = \frac{3m_\nu + N_{\nu_s} m_{\nu_s}}{3 + N_{\nu_s}}. \tag{B2}$$

In other words, these data are not sensitive to mass splittings between different neutrino eigenstates (see, e.g., [48–50]), whether they be active or sterile.

The expressions above can thus be used to explain the constraints that we find in the parameter space (m_ν, m_{ν_s}, N_{ν_s}). In particular, they explain the exact degeneracy between m_ν and m_{ν_s}, as, according to Eq. (B2), these parameters can be varied simultaneously in such a way as to keep the ''observed'' $m_{\rm eff}$ constant.

To test that cosmology only carries relevant information on two neutrino parameters, we consider a ΛCDM cosmology, with active and sterile neutrinos (see [22], and Appendix A for a summary), and the run1 data combination. We first run a MCMC on the model with neutrino parameters ($N_{\rm eff}$, $m_{\rm eff}$), i.e., assuming an $N_{\rm eff}$-fold degeneracy of a neutrino mass eigenstate with mass $m_{\rm eff}$, and imposing a prior $N_{\rm eff} \geq 3$. We then calculate the marginalized constraints on ($N_{\rm eff}$, $m_{\rm eff}$), which we show in the bottom right panel of Fig. 6. Next, we derive constraints on (m_ν, m_{ν_s}, N_{ν_s}), treating the ($N_{\rm eff}$, $m_{\rm eff}$ posterior as a ''measurement.'' More specifically, we sample the (m_ν, m_{ν_s}, N_{ν_s}) parameter space, at each point calculate the corresponding ($N_{\rm eff}$, $m_{\rm eff}$) values, and then use the previously found marginalized posterior as a likelihood. This gives a three-dimensional probability distribution for the sterile-active neutrino parameter space, and we show the marginalized, two-dimensional contours in the remaining panels of Fig. 6 (black contours).

Comparing this to the results obtained in [22] (red contours), we find that the constraints on the active and sterile neutrino masses presented here can indeed be understood very well in terms of cosmological sensitivity to two parameter combinations ($N_{\rm eff}$ and $m_{\rm eff}$). The degeneracy between m_ν and m_{ν_s}, clearly visible in both sets of contours, can thus be explained fully in terms of the dependence of $m_{\rm eff}$ on these two parameters, according to Eq. (B2).

[1] M. C. Gonzalez-Garcia and M. Maltoni, Phys. Rep. **460**, 1 (2008).
[2] J. Lesgourgues and S. Pastor, Phys. Rep. **429**, 307 (2006).
[3] E. Komatsu *et al.* (WMAP Collaboration), Astrophys. J. Suppl. Ser. **192**, 18 (2011).
[4] B. A. Reid, L. Verde, R. Jimenez, and O. Mena, J. Cosmol. Astropart. Phys. 01 (2010) 003.
[5] J. Hamann, S. Hannestad, J. Lesgourgues, C. Rampf, and Y. Y. Y. Wong, J. Cosmol. Astropart. Phys. 07 (2010) 022.
[6] G. Mangano, A. Melchiorri, O. Mena, G. Miele, and A. Slosar, J. Cosmol. Astropart. Phys. 03 (2007) 006.
[7] J. Hamann, S. Hannestad, G. G. Raffelt, and Y. Y. Y. Wong, J. Cosmol. Astropart. Phys. 08 (2007) 021.
[8] G. Mangano, G. Miele, S. Pastor, O. Pisanti, and S. Sarikas, J. Cosmol. Astropart. Phys. 03 (2011) 035.
[9] M. Archidiacono, E. Calabrese, and A. Melchiorri, Phys. Rev. D **84**, 123008 (2011).
[10] A. Aguilar *et al.* (LSND Collaboration), Phys. Rev. D **64**, 112007 (2001).
[11] M. Sorel, J. M. Conrad, and M. Shaevitz, Phys. Rev. D **70**, 073004 (2004).
[12] G. Karagiorgi, A. Aguilar-Arevalo, J. M. Conrad, M. H. Shaevitz, K. Whisnant, M. Sorel, and V. Barger, Phys. Rev. D **75**, 013011 (2007); **80**, 099902 (2009).
[13] A. A. Aguilar-Arevalo *et al.* (The MiniBooNE Collaboration), Phys. Rev. Lett. **98**, 231801 (2007).
[14] A. A. Aguilar-Arevalo *et al.* (MiniBooNE Collaboration), Phys. Rev. Lett. **103**, 111801 (2009).
[15] G. Karagiorgi, Z. Djurcic, J. M. Conrad, M. H. Shaevitz, and M. Sorel, Phys. Rev. D **80**, 073001 (2009); **81**, 039902 (E) (2010).
[16] T. A. Mueller, D. Lhuillier, M. Fallot, A. Letourneau, S. Cormon, M. Fechner, L. Giot, T. Lasserre *et al.*, Phys. Rev. C **83**, 054615 (2011).
[17] G. Mention, M. Fechner, T. Lasserre, T. A. Mueller, D. Lhuillier, M. Cribier, and A. Letourneau, Phys. Rev. D **83**, 073006 (2011).
[18] J. Kopp, M. Maltoni, and T. Schwetz, Phys. Rev. Lett. **107**, 091801 (2011).
[19] A. Melchiorri, O. Mena, S. Palomares-Ruiz, S. Pascoli, A. Slosar, and M. Sorel, J. Cosmol. Astropart. Phys. 01 (2009) 036.
[20] M. A. Acero and J. Lesgourgues, Phys. Rev. D **79**, 045026 (2009).
[21] J. Hamann, S. Hannestad, G. G. Raffelt, I. Tamborra, and Y. Y. Y. Wong, Phys. Rev. Lett. **105**, 181301 (2010).
[22] E. Giusarma, M. Corsi, M. Archidiacono, R. de Putter, A. Melchiorri, O. Mena, and S. Pandolfi, Phys. Rev. D **83**, 115023 (2011).
[23] S. Hannestad, Phys. Rev. Lett. **95**, 221301 (2005).
[24] J. Hamann, S. Hannestad, G. G. Raffelt, and Y. Y. Y. Wong, J. Cosmol. Astropart. Phys. 09 (2011) 034.

[25] E. Calabrese, D. Huterer, E. V. Linder, A. Melchiorri, and L. Pagano, Phys. Rev. D **83**, 123504 (2011).
[26] G. La Vacca, S. A. Bonometto, and L. P. L. Colombo, New Astron. Rev. **14**, 435 (2009).
[27] M. B. Gavela, D. Hernandez, L. L. Honorez, O. Mena, and S. Rigolin, J. Cosmol. Astropart. Phys. 07 (2009) 034; 05 (2010) E01.
[28] J. R. Kristiansen and O. Elgaroy, arXiv:1104.0704 [Astron. Astrophys. (to be published)].
[29] A. Lewis, A. Challinor, and A. Lasenby, Astrophys. J. **538**, 473 (2000).
[30] A. Lewis and S. Bridle, Phys. Rev. D **66**, 103511 (2002).
[31] D. Larson *et al.*, Astrophys. J. Suppl. Ser. **192**, 16 (2011).
[32] B. A. Reid *et al.*, Mon. Not. R. Astron. Soc. **404**, L60 (2010).
[33] A. G. Riess *et al.*, Astrophys. J. **699**, 539 (2009).
[34] R. Amanullah *et al.*, Astrophys. J. **716**, 712 (2010).
[35] E. Aver, K. A. Olive, and E. D. Skillman, J. Cosmol. Astropart. Phys. 05 (2010) 003.
[36] Y. I. Izotov and T. X. Thuan, Astrophys. J. **710**, L67 (2010).
[37] M. Pettini, B. J. Zych, M. T. Murphy, A. Lewis, and C. C. Steidel, arXiv:0805.0594 [Mon. Not. R. Astron. Soc. (to be published)}.
[38] O. Pisanti, A. Cirillo, S. Esposito, F. Iocco, G. Mangano, G. Miele, and P. D. Serpico, Comput. Phys. Commun. **178**, 956 (2008).
[39] J. Hamann, J. Lesgourgues, and G. Mangano, J. Cosmol. Astropart. Phys. 03 (2008) 004.
[40] Z. Hou, R. Keisler, L. Knox, M. Millea, and C. Reichardt, arXiv:1104.2333.
[41] K. Ichikawa, T. Sekiguchi, and T. Takahashi, Phys. Rev. D **78**, 083526 (2008).
[42] M. Chevallier and D. Polarski, Int. J. Mod. Phys. D **10**, 213 (2001).
[43] E. V. Linder, Phys. Rev. Lett. **90**, 091301 (2003).
[44] A. Albrecht, G. Bernstein, R. Cahn, W. L. Freedman, J. Hewitt, W. Hu, J. Huth, and M. Kamionkowski *et al.*, arXiv:astro-ph/0609591.
[45] E. V. Linder, Phys. Rev. D **73**, 063010 (2006).
[46] L. L. Honorez, B. A. Reid, O. Mena, L. Verde, and R. Jimenez, J. Cosmol. Astropart. Phys. 09 (2010) 029.
[47] M. B. Gavela, L. Lopez Honorez, O. Mena, and S. Rigolin, J. Cosmol. Astropart. Phys. 11 (2010) 044.
[48] A. Slosar, Phys. Rev. D **73**, 123501 (2006).
[49] F. de Bernardis, T. Kitching, A. Heavens, and A. Melchiorri, Phys. Rev. D **80**, 123509 (2009).
[50] R. Jimenez, T. Kitching, C. Pena-Garay, and L. Verde, J. Cosmol. Astropart. Phys. 05 (2010) 035.